

Supplementary Information

Excited-state structure of copper phenanthroline-based photosensitizers

Alexander Guda, Johannes Windisch, Benjamin Probst, Jeroen A. van Bokhoven, Roger Alberto, Maarten Nachtegaal, Lin X. Chen, Grigory Smolentsev

Synthesis of 2,9-di-*sec*-butyl-3,4,7,8-tetramethyl-1,10-phenanthroline (dsbtmp)

In a 25 mL Schlenk flask 3,4,7,8-tetramethyl-1,10-phenanthroline was dissolved in dry toluene (7 mL). At 0 °C *s*-BuLi (1.3 M in hexane, 3.59 mL, 4.67 mmol) was added dropwise to give a deep red solution. After stirring at rt for 3 h, the reaction was quenched by the dropwise addition of degassed water (5 mL) at 0 °C. The layers were separated, the aqueous layer was extracted with DCM (3x 20 mL) and the combined organic layers were washed with water. To the bright yellow organic layer MnO₂ (8 g) was added and the suspension was stirred until decoloration was observed. MgSO₄ was added for drying, the mixture was filtered over celite and the filtrate was concentrated under reduced pressure. The crude product was purified by column chromatography (neutral alumina, DCM, 0.5% MeOH, 0.5% TEA) to give the pure product as a colorless solid (518 mg, 1.49 mmol, 70%).

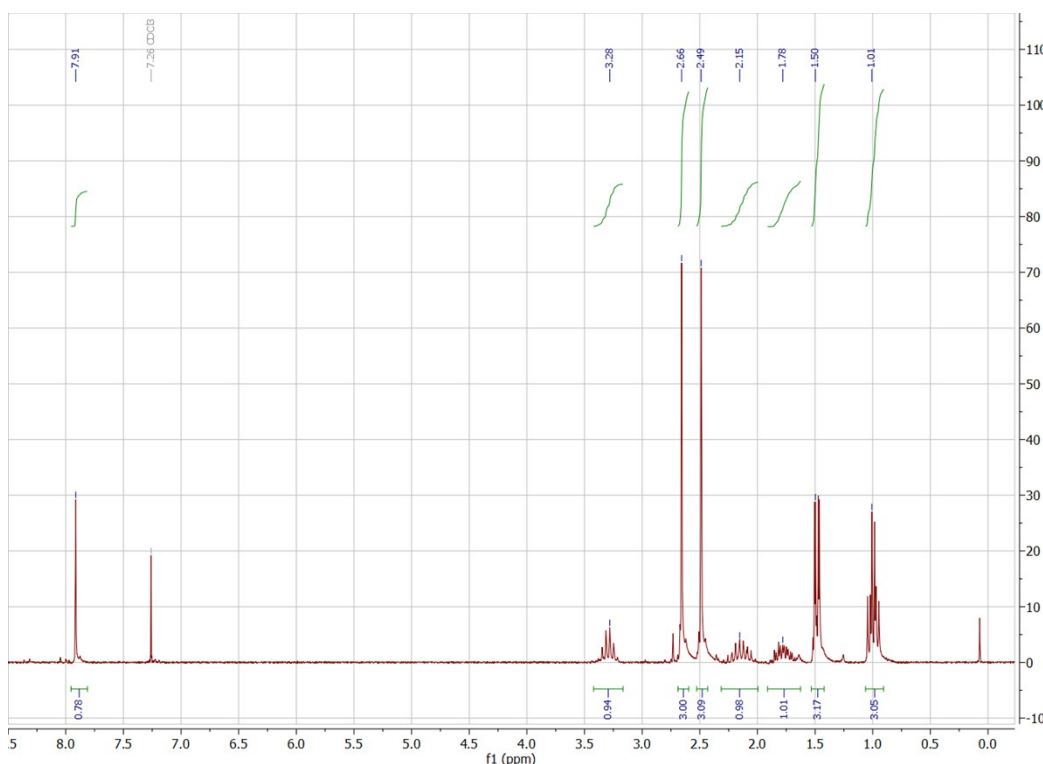
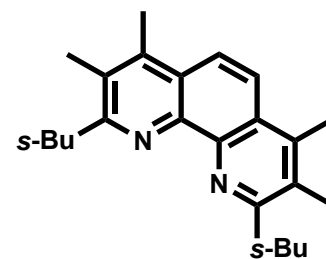


Figure S1. ¹H-NMR of dsbtmp in CDCl₃ (200 MHz).

$^1\text{H NMR}$ (200 MHz, CDCl_3): δ 7.91 (s, 2H), 3.28 (sext, $J = 6.6$ Hz, 2H), 2.66 (s, 6H), 2.49 (s, 6H), 2.18-1.61 (m, 4H), 1.40 (dd, $J = 6.8, 1.6$ Hz, 6H), 0.91 (td, $J = 7.4, 4.8$ Hz, 6H); **ESI-MS**: $m/z = 349.3$ $[\text{M}+\text{H}]^+$ (100%).

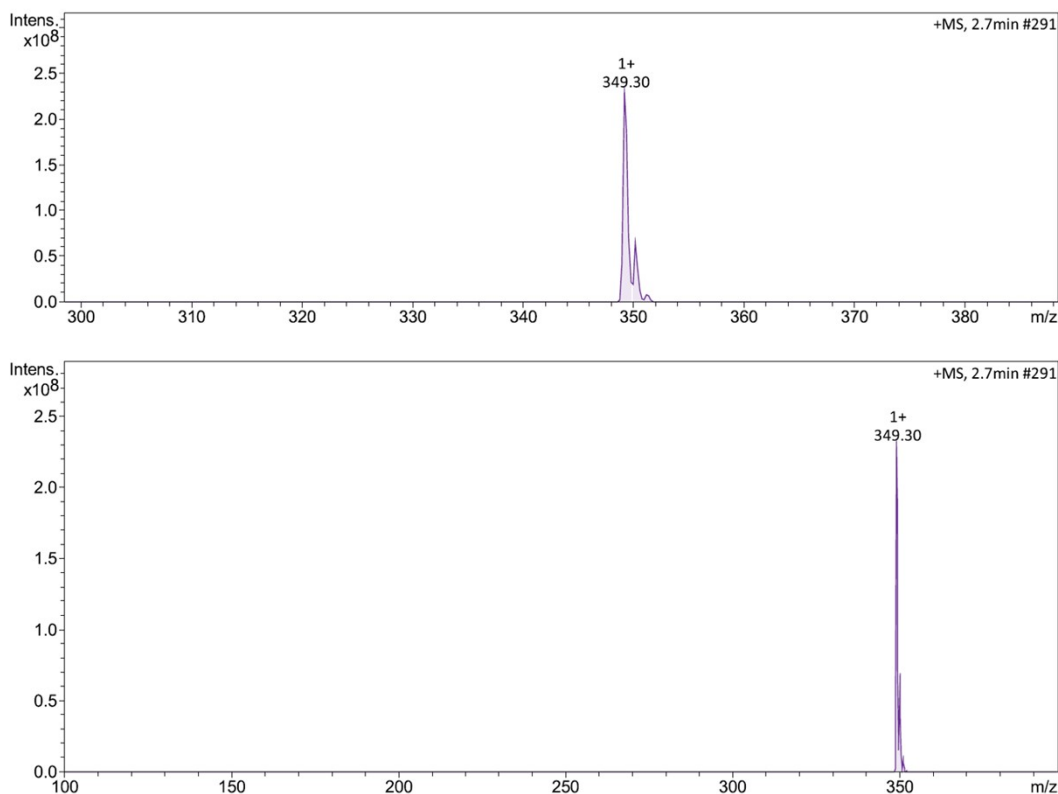
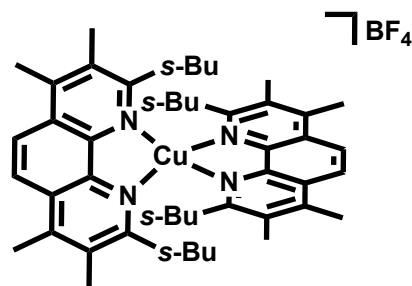


Figure S2. ESI-MS of dsbtmp.

Synthesis of $[\text{Cu}(\text{dsbtmp})_2]\text{BF}_4$

A 100 mL Schlenk flask was charged with $[\text{Cu}(\text{MeCN})_4]\text{BF}_4$ (406 mg, 1.29 mmol) and 2,9-di-*sec*-butyl-3,4,7,8-tetramethyl-1,10-phenanthroline (900 mg, 2.58 mmol). Upon addition of DCM (5 mL) a dark red solution formed, which was stirred at room temperature for 1 h. Et_2O (50 mL) was added which led to the precipitation of an orange solid. The precipitate was filtered off, was washed with Et_2O and dried under HV to give the pure product as an orange powder (874 mg, 1.03 mmol, 80%).



$^1\text{H NMR}$ (300 MHz, CDCl_3): δ 8.21 (s, 4H), 3.68-3.12 (m, 4H), 2.82-2.76 (m, 12H), 2.57-2.48 (m, 12H), 1.50-1.20 (m, 8H), 1.12-0.76 (m, 12H), 0.21 to -0.18 (m, 12H); **ESI-MS**: $m/z = 759.5$ $[\text{M}-\text{BF}_4]^+$ (100%); **Anal. calcd.** for $\text{C}_{48}\text{H}_{64}\text{BCuF}_4\text{N}_4$ (%): C: 68.03, H: 7.61, N: 6.61; Found: C: 67.76, H: 7.42, N: 6.55.

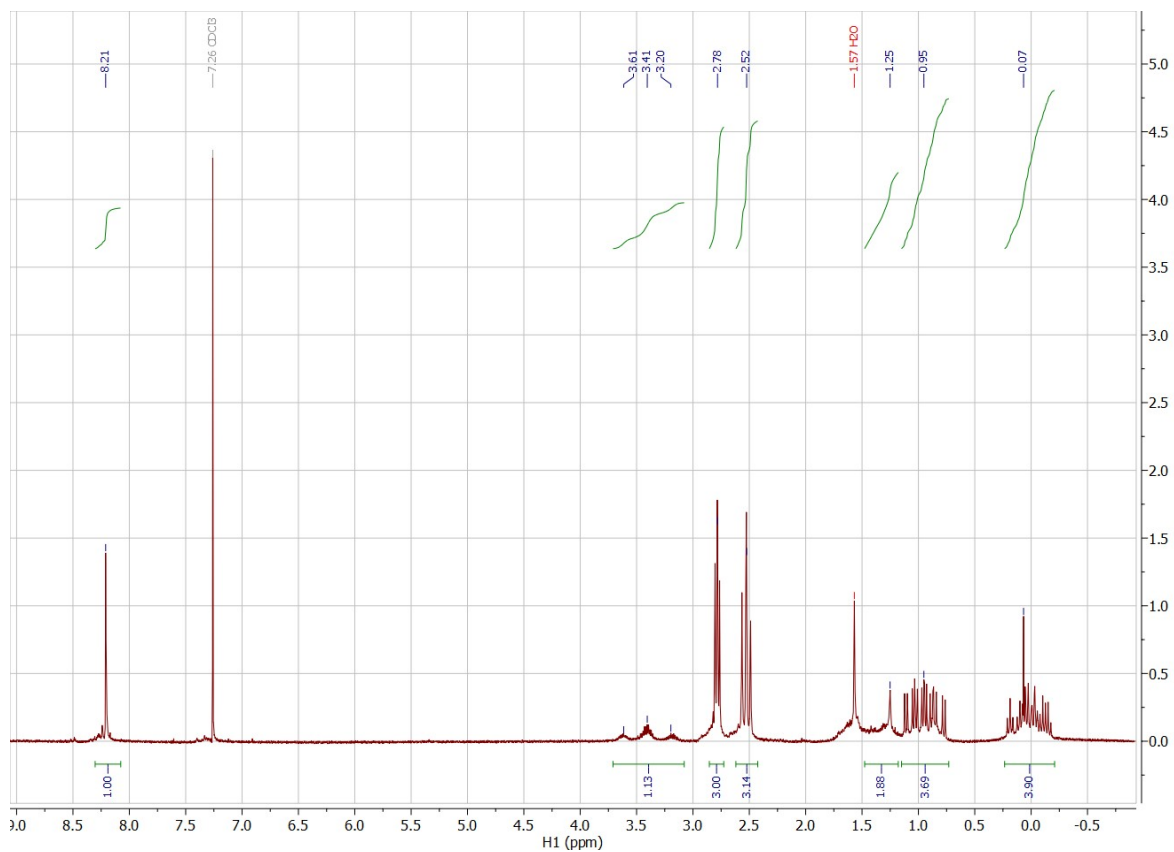


Figure S3. $^1\text{H-NMR}$ of $[\text{Cu}(\text{dsbtmp})_2]\text{BF}_4$ in CDCl_3 (300 MHz).

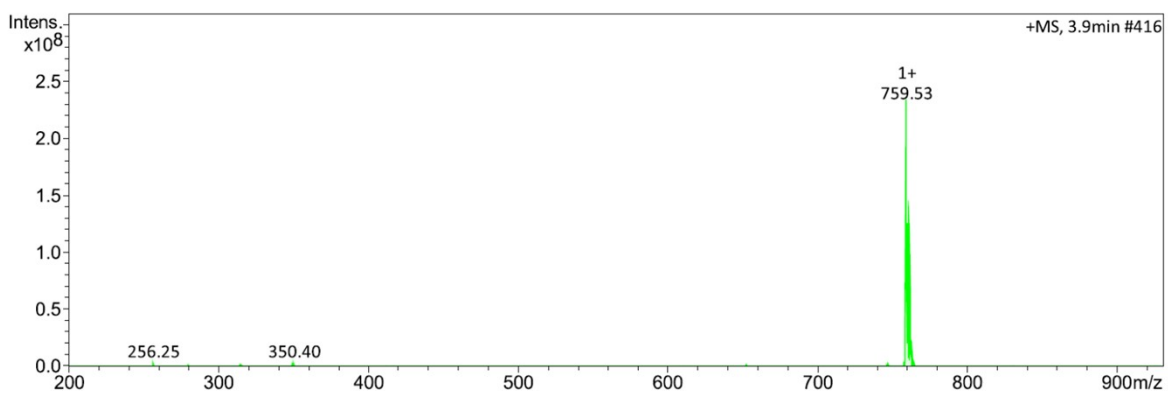
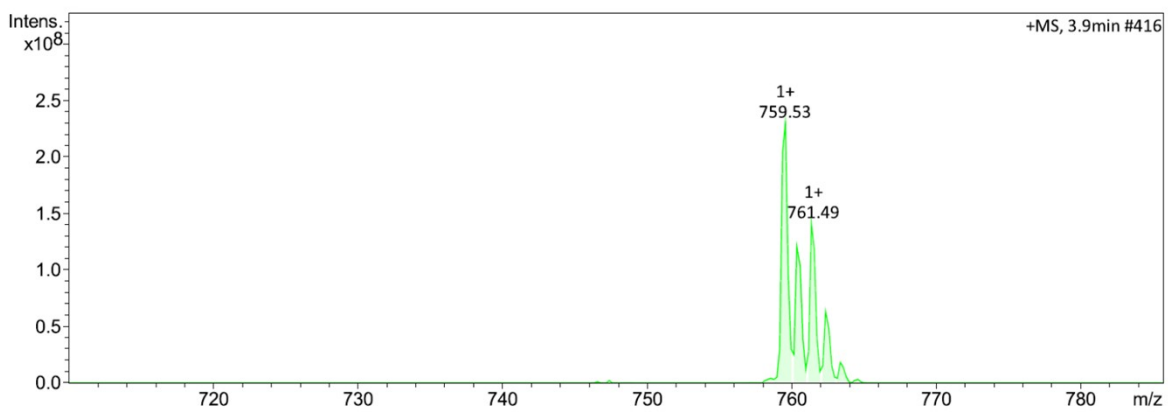


Figure S4. ESI-MS of $[\text{Cu}(\text{dsbtmp})_2]\text{BF}_4$.

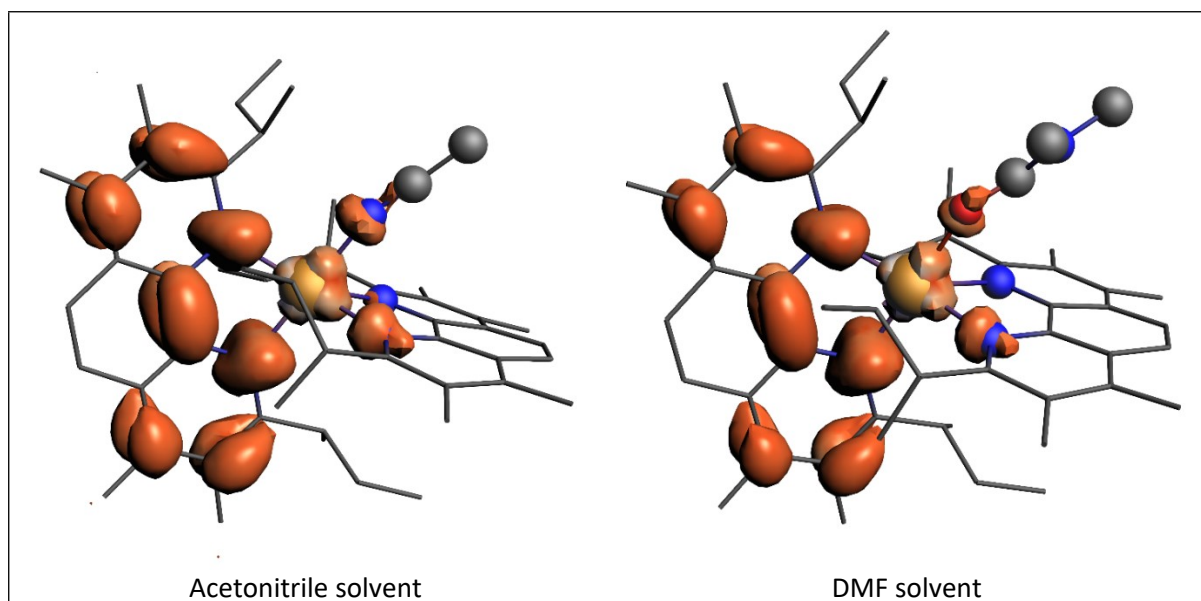


Figure S5. DFT-optimized structures of the exciplex state of $[\text{Cu}(\text{dsbtmp})_2]^+$ with a bond between solvent molecule and the Cu center. The structure 3c with DMF as a solvent is shown on the right and the analogous structure with acetonitrile is shown on the left. Atoms of solvents, Cu and nearest to the metal N atoms are shown as balls, other atoms are plotted with sticks. Cu atom is yellow, C atoms are gray, N atoms are blue, H atoms are not shown. Spin density is shown as isosurfaces.

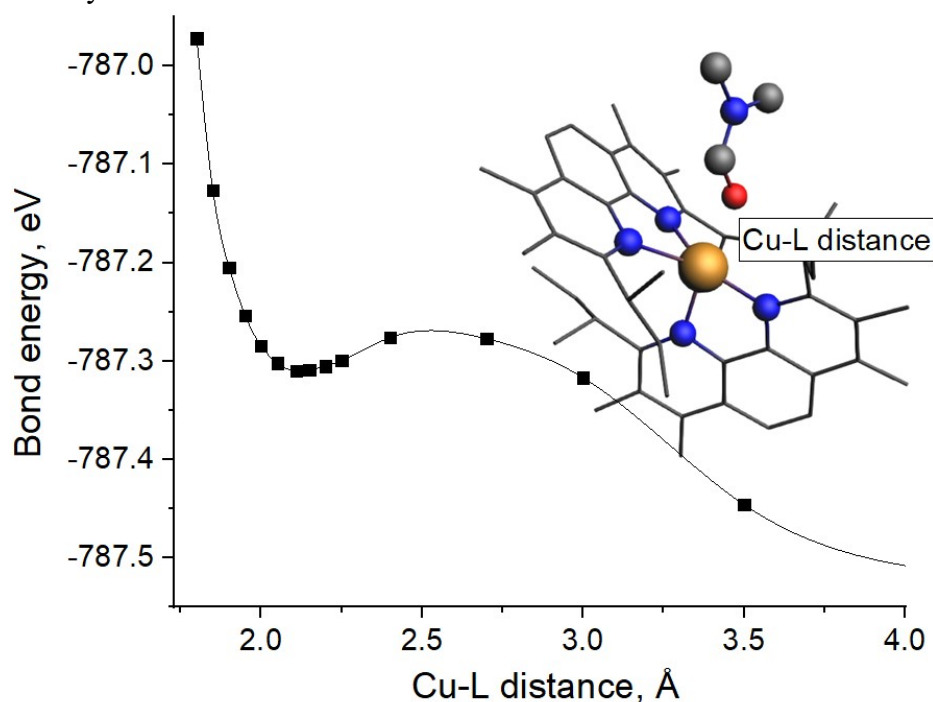


Figure S6. The energy of the triplet excited state of the $[\text{Cu}(\text{dsbtmp})_2]^+$ -DMF exciplex (3c) obtained using DFT for relaxed geometries with constrained distances between Cu and DMF. Calculations were performed using ADF code with TZP basis set for geometry optimization and TZ2P basis set for total energy calculation. All energies were corrected by 1.00 eV to enable direct comparison with $[\text{Cu}(\text{dmp})_2]^+$ data obtained using the QZ4P basis set. When calculating the bond energy for complexes with a solvent molecule the bonding energy of the latter was subtracted from the total value (-78.40 eV).

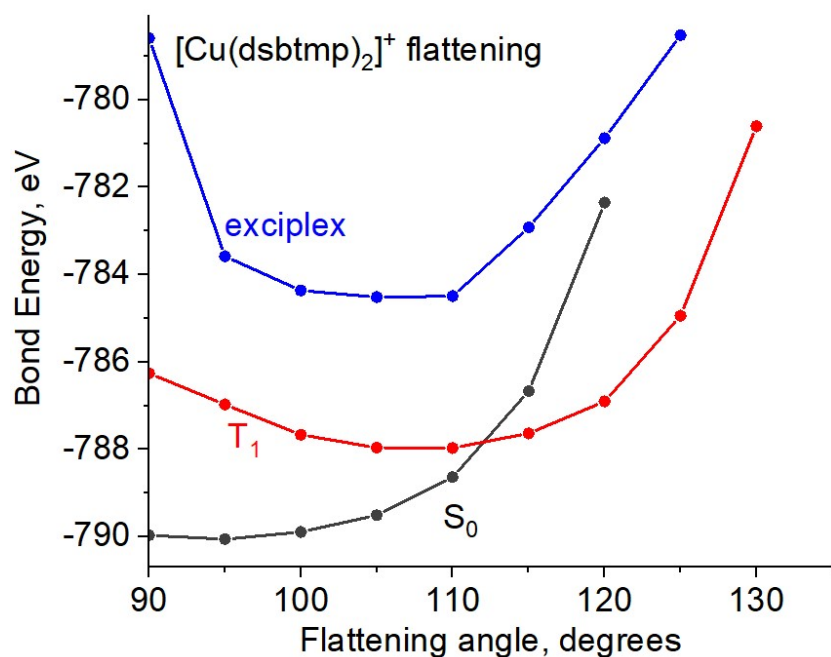


Figure S7. The cross-section of the potential energy surfaces for singlet (3a), triplet (3b) and exciplex (3c) states of the $[\text{Cu}(\text{dsbtmp})_2]^+$ molecule along the flattening angle. Calculations were performed using ADF code with TZ2P basis set for total energy calculation. All energies were corrected by 1.00 eV to enable direct comparison with $[\text{Cu}(\text{dmp})_2]^+$ data obtained using the QZ4P basis set. When calculating the bond energy for complexes with a solvent molecule the bonding energy of the latter was subtracted from the total value (-78.40 eV). The distance between Cu and O atom of DMF was set at 2.13 Å for the exciplex state.

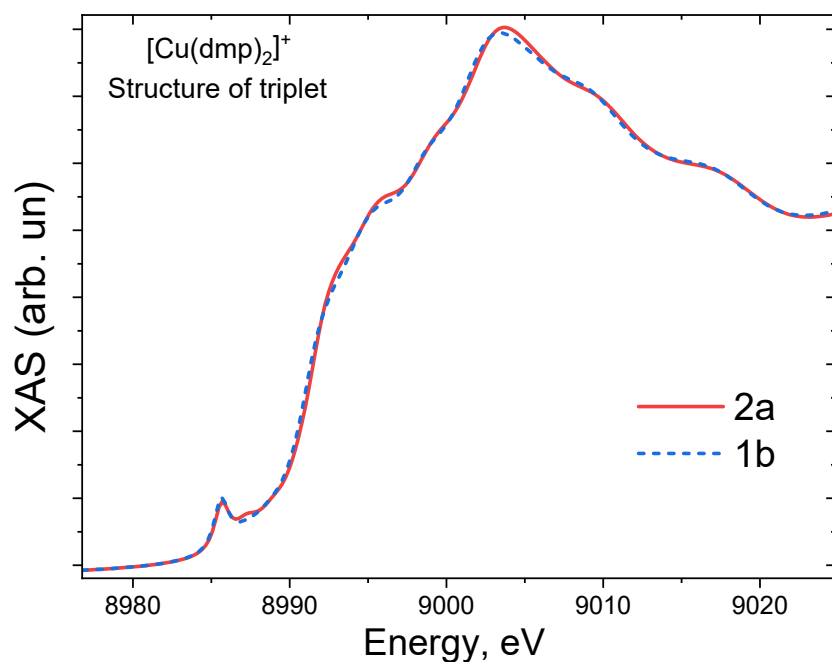


Figure S8. Theoretical XANES spectra of $[\text{Cu}(\text{dmp})_2]^+$ calculated for the same structure, corresponding to the triplet MLCT state. Electron is located at the ligand (triplet MLCT state, 1b) or completely removed from the complex (electrochemically generated state, 2a)

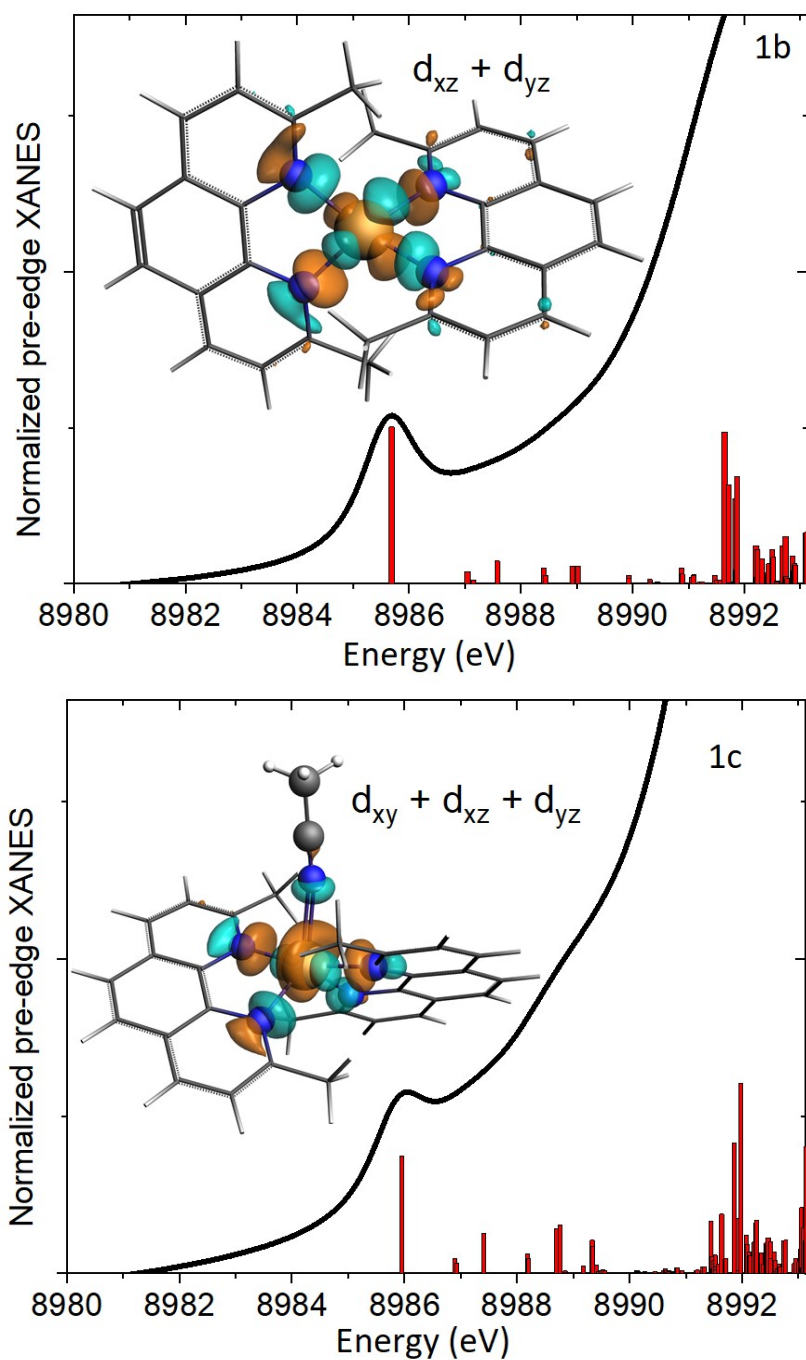


Figure S9. Calculated X-ray absorption spectra in the pre-edge region for $[\text{Cu}(\text{dmp})_2]^+$ in the triplet state (1b, top panel) and in the exciplex state with Cu-acetonitrile distance 2.33\AA (1c, bottom panel) and molecular orbitals that give the dominant contribution to the pre-edge peak.

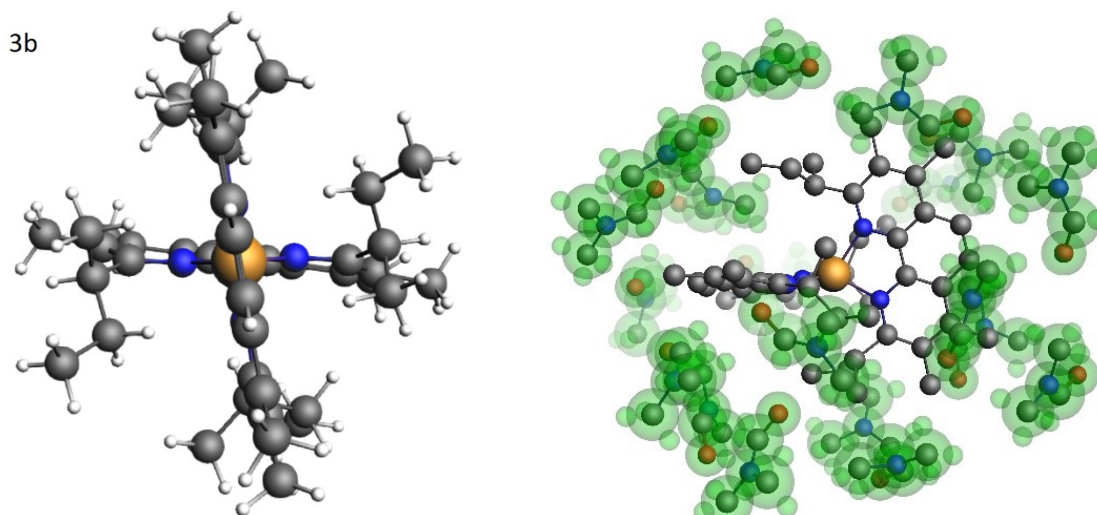


Figure S10. Structure of $[\text{Cu}(\text{dsbtmp})_2]^+$ in the triplet MLCT state (3b) in a gas phase, where dimethylformamide solvent is simulated as a dielectric medium within the COSMO model (left panel), and with explicit solvent molecules surrounding the complex (right panel). Solvent molecules are marked by green.

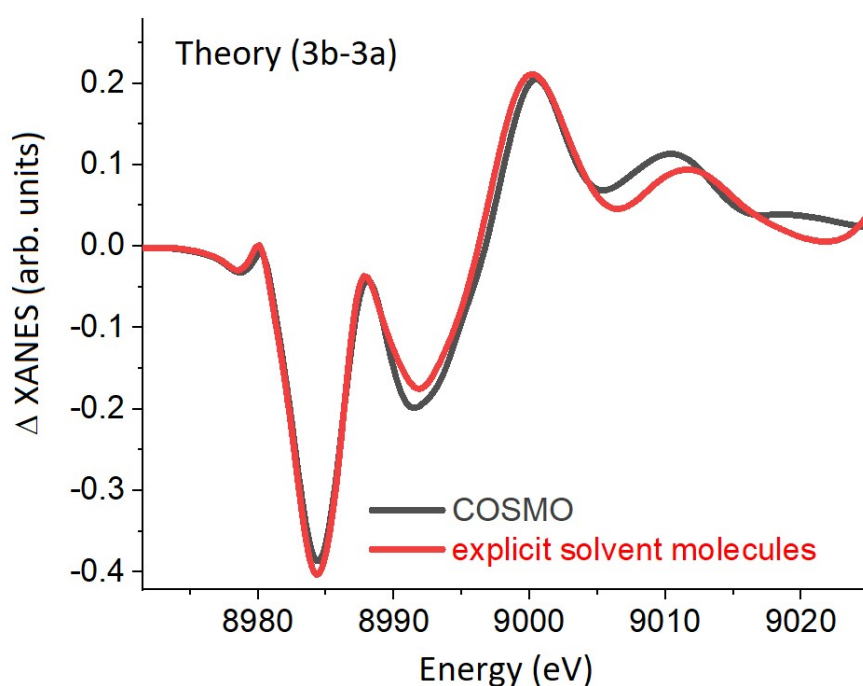


Figure S11. Theoretical Cu K-edge difference XANES spectra between triplet and singlet configurations of $[\text{Cu}(\text{dsbtmp})_2]^+$ (3b-3a) calculated for the structures optimized in dielectric medium (figure S8, left panel) and surrounded by explicit solvent molecules (figure S10, right panel). The difference spectra are almost insensitive to the non-coordinating solvation shell around Cu complex and thus COSMO model is a good enough approximation for the comparison with experimental data.

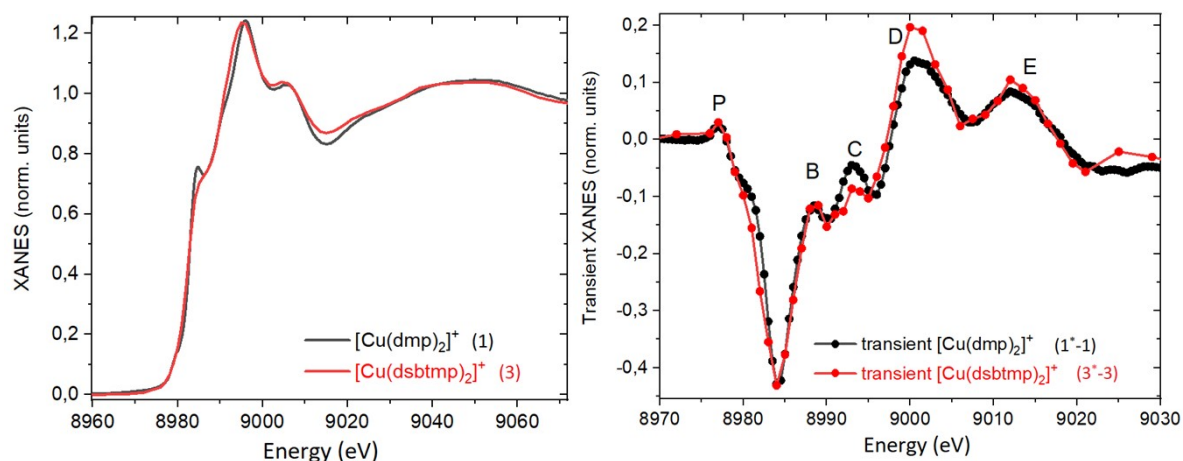


Figure S12. Left panel: experimental ground state spectra of $[\text{Cu}(\text{dmp})_2]^+$ in acetonitrile (1) and $[\text{Cu}(\text{dsbtmp})_2]^+$ in DMF (3). Right panel: experimental pump-probe signals for $[\text{Cu}(\text{dmp})_2]^+$ in acetonitrile (1*-1) and $[\text{Cu}(\text{dsbtmp})_2]^+$ in DMF (3*-3).

Supplementary tables

Table S1. Geometry parameters for the DFT optimized $[\text{Cu}(\text{dmp})_2]^+$, $[\text{Cu}(\text{dmp})_2]^{2+}$, $[\text{Cu}(\text{dsbtmp})_2]^+$ structures in singlet, triplet states and after coordination by solvent molecule. When calculating the bond energy for complexes with a solvent molecule the bonding energy of the latter was subtracted from the total value (-42.49 eV for MeCN and -78.40 for DMF).

Complex	Spin state	Solvent coordination	DFT model	Energy	Cu-Solvent	Average Cu-N	Flattering angle
$[\text{Cu}(\text{dmp})_2]^+$	Singlet	No	1a	-422.07	∞	2.07	90
$[\text{Cu}(\text{dmp})_2]^+$	Triplet	No	1b	-420.32	∞	1.95 \times 2 2.07 \times 2	111
$[\text{Cu}(\text{dmp})_2]^+$	Triplet	Yes (MeCN)	1c	-419.99	2.3	2,07	119
$[\text{Cu}(\text{dmp})_2]^{2+}$	Doublet	No	2a	-417.33	∞	2.01	112
$[\text{Cu}(\text{dmp})_2]^{2+}$	Doublet	Yes (MeCN)	2b	-417.22	2.12	2.09	119
$[\text{Cu}(\text{dsbtmp})_2]^+$	Singlet	No	3a	-790.10	∞	2,08	98
$[\text{Cu}(\text{dsbtmp})_2]^+$	Triplet	No	3b	-788.04	∞	1.98 \times 2 2.07 \times 2	105
$[\text{Cu}(\text{dsbtmp})_2]^+$	Triplet	Yes (DMF)	3c	-787,31	2.11	2.16	105
$[\text{Cu}(\text{dsbtmp})_2]^+$	Triplet	Yes (MeCN)	3d	-787,30	2.07	2.16	103

Table S2. Contribution Cu 3d and 4p states into molecular orbital that forms the pre-edge peak of XANES spectrum

	Cu-solvent distance	Cu 4p %	Cu 3d %
Triplet	∞	6.66	55.1
Exciplex*	2.33	1.45	60.4
	2.23	1.02	60.8
	2.13	<1	61.0
	2.03	<1	60.7

* All exciplex structures have the same coordinates (geometry optimization with Cu-N = 2.33) and only distance Cu-solvent was manually changed.

Supplementary references

- [1] G. Smolentsev, A. A. Guda, M. Janousch, C. Frieh, G. Jud, F. Zamponi, M. Chavarot-Kerlidou, V. Artero, J. A. van Bokhoven, M. Nachttegaal, *Faraday Discuss.* **2014**, *171*, 259–273.
- [2] C. E. McCusker, F. N. Castellano, *Inorg. Chem.* **2013**, *52*, 8114–8120.
- [3] L. X. Chen, G. B. Shaw, I. Novozhilova, T. Liu, G. Jennings, K. Attenkofer, G. J. Meyer, P. Coppens, *J. Am. Chem. Soc.* **2003**, *125*, 7022–7034.
- [4] M. S. Kelley, M. L. Shelby, M. W. Mara, K. Haldrup, D. Hayes, R. G. Hadt, X. Zhang, A. B. Stickrath, R. Ruppert, J.-P. Sauvage, D. Zhu, H. T. Lemke, M. Chollet, G. C. Schatz, L. X. Chen, *J. Phys. B-At. Mol. Opt. Phys.* **2017**, *50*, 154006.
- [5] C. F. Guerra, J. G. Snijders, G. te Velde, E. J. Baerends, *Theor. Chem. Acc.* **1998**, *99*, 391–403.
- [6] G. te Velde, F. M. Bickelhaupt, E. J. Baerends, C. Fonseca Guerra, S. J. A. van Gisbergen, J. G. Snijders, T. Ziegler, *J. Comput. Chem.* **2001**, *22*, 931–967.
- [7] M. Reiher, O. Salomon, B. Artur Hess, *Theor. Chem. Acc.* **2001**, *107*, 48–55.
- [8] A. Klamt, G. Schüürmann, *J. Chem. Soc. Perkin Trans. 2* **1993**, 799–805.
- [9] M. Tromp, A. J. Dent, J. Headspith, T. L. Easun, X.-Z. Sun, M. W. George, O. Mathon, G. Smolentsev, M. L. Hamilton, J. Evans, *J. Phys. Chem. B* **2013**, *117*, 7381–7387.
- [10] I. Alperovich, G. Smolentsev, D. Moonshiram, J. W. Jurss, J. J. Concepcion, T. J. Meyer, A. Soldatov, Y. Pushkar, *J. Am. Chem. Soc.* **2011**, *133*, 15786–15794.